

Generalization Evaluation of Deep Stereo Matching Methods for UAV-Based Forestry Applications

Yida Lin, Bing Xue, Mengjie Zhang

Centre for Data Science and Artificial Intelligence

Victoria University of Wellington, Wellington, New Zealand

linyida@myvuw.ac.nz, bing.xue@vuw.ac.nz, mengjie.zhang@vuw.ac.nz

Sam Schofield, Richard Green

Department of Computer Science and Software Engineering

University of Canterbury, Canterbury, New Zealand

sam.schofield@canterbury.ac.nz, richard.green@canterbury.ac.nz

Abstract—Autonomous UAV forestry operations require robust depth estimation methods with strong cross-domain generalization. However, existing evaluations focus on urban and indoor scenarios, leaving a critical gap for specialized vegetation-dense environments. We present the first systematic zero-shot evaluation of eight state-of-the-art stereo methods—RAFT-Stereo, IGEV, IGEV++, BridgeDepth, StereoAnywhere, DEFOM (plus baseline methods ACVNet, PSMNet, TCstereo)—spanning iterative refinement, foundation model, and zero-shot adaptation paradigms. All methods are trained exclusively on Scene Flow and evaluated without fine-tuning on four standard benchmarks (ETH3D, KITTI 2012/2015, Middlebury) plus a novel 5,313-pair Canterbury forestry dataset captured with ZED Mini camera (1920×1080). Performance reveals scene-dependent patterns: foundation models excel on structured scenes (BridgeDepth: 0.23 px on ETH3D, 0.83-1.07 px on KITTI; DEFOM: 0.35-4.65 px across benchmarks), while iterative methods maintain cross-domain robustness (IGEV++: 0.36-6.77 px; IGEV: 0.33-21.91 px). Critical finding: RAFT-Stereo exhibits catastrophic ETH3D failure (26.23 px EPE, 98% error rate) due to negative disparity predictions, while performing normally on KITTI (0.90-1.11 px). Qualitative evaluation on Canterbury forestry dataset identifies DEFOM as the optimal gold-standard baseline for vegetation depth estimation, exhibiting superior depth smoothness, occlusion handling, and cross-domain consistency compared to IGEV++, despite IGEV++’s finer detail preservation.

Index Terms—Stereo matching, depth estimation, generalization evaluation, UAV applications, autonomous forestry

I. INTRODUCTION

Forestry UAVs require robust depth perception for safety-critical tasks including tree health assessment, automated pruning, and autonomous navigation [14], [15]. Unlike urban or indoor scenes, forest canopies feature thin overlapping branches, repetitive patterns, extreme depth discontinuities, and dramatic illumination variations. Stereo vision provides a passive, lightweight alternative to power-hungry active sensors, ideal for resource-constrained aerial platforms.

Deep learning has revolutionized stereo matching, with convolutional and recurrent architectures trained on large-scale synthetic datasets like Scene Flow [1] achieving remarkable accuracy. However, deploying these models in specialized real-world applications presents a fundamental challenge: how to select the most robust method with superior generalization capability across diverse domains? For safety-critical UAV operations, establishing a gold standard baseline through systematic cross-domain evaluation is essential before deployment. The domain gap between synthetic training data and

real deployment scenarios—characterized by different scene statistics, camera parameters, lighting conditions, and object distributions—requires careful empirical validation.

Three critical gaps limit deployment in specialized domains. *First*, evaluations focus on automotive (KITTI [10]) and indoor (Middlebury [12], ETH3D [13]) scenarios, providing limited insight for vegetation-dense environments. *Second*, most studies permit domain-specific fine-tuning, obscuring pure generalization capability and requiring expensive target domain labels. *Third*, relative performance of recent paradigms—iterative refinement, foundation models, zero-shot adaptation—remains unclear for cross-domain deployment. Zero-shot evaluation provides the strongest test of inherent robustness when target labels are unavailable.

We address these gaps by evaluating eight state-of-the-art methods spanning iterative refinement (RAFT-Stereo [2], IGEV [3], IGEV++ [4], CREStereo [5]), foundation models (BridgeDepth [6], FoundationStereo [7]), and zero-shot adaptation (StereoAnywhere [8], ZeroStereo [9]). All methods are trained on Scene Flow and evaluated on four standard benchmarks (ETH3D, KITTI 2012/2015, Middlebury) plus a novel 5,313-pair Canterbury forestry dataset captured with ZED Mini stereo camera (1920×1080). Our contributions are:

- **Systematic paradigm comparison:** First zero-shot evaluation comparing iterative refinement, foundation models, and zero-shot adaptation to isolate inherent generalization capability without domain-specific fine-tuning.
- **Comprehensive cross-domain evaluation:** Testing on four standard datasets (ETH3D, KITTI 2012/2015, Middlebury) spanning indoor, automotive, and high-resolution scenarios with consistent Scene Flow training protocol.
- **Detailed performance analysis:** Quantitative comparison revealing scene-dependent patterns—foundation models excel on structured scenes (BridgeDepth: 0.229 px on ETH3D), iterative methods show variable robustness (IGEV++: 7.82% D1 on Middlebury vs. IGEV: 20.57%), and critical anomaly detection (RAFT-Stereo: 98% ETH3D failure).
- **Deployment guidelines:** Evidence-based recommendations identifying optimal methods for different UAV scenarios (indoor navigation, automotive, safety-critical) with accuracy-robustness trade-off analysis and multi-

benchmark validation requirements.

II. RELATED WORK

A. Classical Stereo Matching

Traditional stereo matching methods follow a four-step pipeline: matching cost computation, cost aggregation, disparity optimization, and disparity refinement [16]. Local methods aggregate costs within fixed windows, offering computational efficiency but struggling with textureless regions and occlusions. Global methods formulate stereo matching as energy minimization problems, employing techniques like graph cuts [17] or belief propagation [18] to enforce smoothness constraints. Semi-global matching (SGM) [19] provides a practical middle ground, aggregating costs along multiple 1D paths to approximate 2D smoothness with reasonable computational cost. While these classical approaches offer interpretability and predictable behavior, they typically require extensive parameter tuning and struggle with complex scenes.

B. Deep Learning for Stereo Matching

Deep learning has transformed stereo matching through end-to-end trainable architectures. Early works like DispNet [1] and GC-Net [20] demonstrated that CNNs could learn robust matching costs and regularization directly from data. PSMNet [21] introduced spatial pyramid pooling for multi-scale context aggregation, while GANet [22] incorporated attention mechanisms for adaptive feature refinement. These pioneering methods established the paradigm of learning-based cost volume construction and 3D aggregation.

Recent advances leverage iterative refinement strategies inspired by optical flow estimation. RAFT-Stereo [2] adapts recurrent all-pairs field transforms from optical flow, achieving state-of-the-art accuracy through iterative updates on multi-scale 4D correlation volumes. Building upon this foundation, IGEV [3] combines iterative updates with explicit geometry encoding to improve depth consistency, while IGEV++ [4] extends this with enhanced feature extraction and unified multi-scale processing for flow, stereo, and depth estimation. CREStereo [5] employs cascaded recurrent refinement for efficient high-resolution processing, achieving favorable accuracy-speed trade-offs.

More recently, foundation model approaches have emerged to exploit large-scale pre-training. BridgeDepth [6] leverages pre-trained monocular depth priors to improve stereo estimation, bridging single-view and two-view geometry. FoundationStereo [7] builds upon large-scale pre-training across diverse datasets for robust zero-shot generalization. StereoAnywhere [8] and ZeroStereo [9] explore meta-learning and diffusion-based paradigms for improved cross-domain transfer without fine-tuning. Despite these architectural innovations, systematic comparative evaluation of generalization capabilities across diverse real-world domains—particularly specialized applications like forestry—remains limited in existing literature.

C. Stereo Vision in UAV Applications

UAV-based stereo vision has been explored for various applications including autonomous navigation [23], 3D reconstruction [24], and obstacle avoidance [25]. However, most systems focus on urban or structured environments. Forestry applications present unique challenges: dense foliage creates ambiguous correspondences, variable lighting causes appearance changes, and thin branch structures require fine-grained depth resolution. While monocular depth estimation has been applied to forest inventory [26], stereo-based approaches for autonomous forestry operations remain underexplored.

D. Generalization in Stereo Matching

Domain adaptation for stereo matching typically employs supervised fine-tuning on target domains [27] or self-supervised adaptation using photometric consistency [28]. While effective, these approaches require target domain data and computational resources for retraining. Zero-shot generalization—deploying models trained solely on synthetic data to real-world scenarios without adaptation—remains challenging. The Scene Flow dataset [1], comprising synthetic imagery with perfect ground truth, has become the de facto standard for pre-training. However, systematic evaluation of Scene Flow-trained models across multiple real-world domains, particularly specialized applications like forestry, has received limited attention. Our work addresses this gap through comprehensive cross-domain evaluation.

III. METHODOLOGY

A. Problem Formulation

Stereo matching estimates per-pixel disparity from a rectified stereo image pair. Given left and right images $I_L, I_R \in \mathbb{R}^{H \times W \times 3}$, the goal is to compute a disparity map $D \in \mathbb{R}^{H \times W}$ where each pixel (x, y) in the left image corresponds to pixel $(x - D(x, y), y)$ in the right image. The depth Z at pixel (x, y) can be recovered through triangulation:

$$Z(x, y) = \frac{f \cdot B}{D(x, y)} \quad (1)$$

where f is the focal length and B is the stereo baseline. Deep stereo methods learn a mapping $f_\theta : \mathbb{R}^{H \times W \times 3} \times \mathbb{R}^{H \times W \times 3} \rightarrow \mathbb{R}^{H \times W}$ parameterized by weights θ , trained to minimize disparity prediction error on labeled data.

B. Datasets

We evaluate stereo matching methods across five diverse datasets to assess generalization capability:

Scene Flow [1] provides 39,000+ synthetic stereo pairs with perfect ground truth for training all evaluated methods.

ETH3D [13] contains high-resolution indoor/outdoor pairs with structured light ground truth, emphasizing geometric accuracy.

KITTI 2012/2015 [10], [11] represent autonomous driving with LiDAR ground truth. KITTI 2015 adds dynamic objects and occlusion challenges.

Middlebury [12] provides high-accuracy indoor ground truth testing fine-grained disparity estimation.

Canterbury Forestry Dataset: 5,313 stereo pairs (1920×1080) captured using ZED Mini stereo camera in Canterbury, New Zealand forest sites (March-October 2024). Selected from hundreds of thousands of captured pairs, this dataset targets vegetation-specific challenges absent in standard benchmarks: thin branches (3-8cm diameter), repetitive foliage patterns, extreme depth discontinuities (>10m), and variable natural illumination. The dataset serves as a zero-shot evaluation testbed—*no ground truth depth maps are provided*, enabling assessment of pure cross-domain generalization from Scene Flow training to real-world forestry conditions. Qualitative results demonstrate method robustness on challenging vegetation scenes. Dataset will be publicly released.

C. Evaluated Stereo Matching Methods

We evaluate eight representative deep stereo matching methods spanning different architectural paradigms, as summarized in Table I. All methods are trained on Scene Flow and evaluated without any fine-tuning to assess pure zero-shot generalization capability.

TABLE I: Evaluated Stereo Matching Methods

Method	Type
RAFT-Stereo [2]	Iterative
CREStereo [5]	Cascaded
IGEV [3]	Iterative
IGEV++ [4]	Iterative
BridgeDepth [6]	Foundation
FoundationStereo [7]	Foundation
StereoAnywhere [8]	Zero-shot
ZeroStereo [9]	Zero-shot

D. Evaluation Metrics

We employ four widely-used metrics to evaluate stereo matching performance:

End-Point Error (EPE) measures the average absolute disparity error:

$$\text{EPE} = \frac{1}{N} \sum_{i=1}^N |d_i - \hat{d}_i| \quad (2)$$

where d_i is the ground truth disparity, \hat{d}_i is the predicted disparity, and N is the number of valid pixels.

D1-Error computes the percentage of pixels with disparity error exceeding 3 pixels:

$$\text{D1} = \frac{1}{N} \sum_{i=1}^N \mathbb{I}(|d_i - \hat{d}_i| > 3) \quad (3)$$

3-Pixel Error (3PE) measures the percentage of predictions with error greater than 3 pixels, similar to D1-Error but often reported separately for all regions, non-occluded regions, and occluded regions.

Root Mean Squared Error (RMSE) provides sensitivity to large errors:

$$\text{RMSE} = \sqrt{\frac{1}{N} \sum_{i=1}^N (d_i - \hat{d}_i)^2} \quad (4)$$

E. Implementation Details

Training Configuration: All methods trained identically on Scene Flow (35,454 training, 4,370 validation pairs) for 200k iterations using AdamW ($\beta_1=0.9$, $\beta_2=0.999$, weight decay 10^{-4}), learning rate 4×10^{-4} with exponential decay ($\gamma=0.85$) every 50k iterations, batch size 8 across 4 GPUs. Images cropped to 384×768. Augmentation [3]: photometric (brightness/contrast/saturation [0.6, 1.4], hue ± 0.1 , gamma [0.8, 1.2]), geometric (flipping $p=0.5$, scaling [0.8, 1.2], rotation $\pm 10^\circ$), random erasing ($p=0.5$, area [0.02, 0.4]). Iterative methods use exponentially increasing supervision weights (0.5, 0.7, 0.9, 1.0). Training stabilizes within 150-200k iterations, verified across three independent runs.

Evaluation Protocol: For evaluation, we use full-resolution images without cropping or resizing to preserve geometric accuracy. Invalid pixels (occluded regions, image boundaries) are excluded from metric computation following standard protocols. We report mean and standard deviation across three random weight initializations to ensure statistical reliability. All experiments are conducted on NVIDIA A100 GPUs with CUDA 11.8 and PyTorch 2.0.

Canterbury Forestry Dataset Acquisition: Stereo pairs are captured using ZED Mini stereo camera (1920×1080 resolution, 12cm baseline, global shutter, hardware-synchronized) in Canterbury, New Zealand forest sites. Data collection spans March-October 2024, capturing diverse natural conditions: sunny/overcast/dappled lighting, morning/afternoon acquisitions, and varying vegetation densities. From hundreds of thousands of captured pairs, 5,313 high-quality pairs are selected based on image clarity, disparity coverage, and vegetation complexity. Unlike standard benchmarks with ground truth depth maps, this dataset serves as a *zero-shot evaluation testbed*—methods trained solely on Scene Flow are directly evaluated on real forestry imagery without fine-tuning or ground truth supervision. This protocol tests pure cross-domain generalization capability, with qualitative assessment focusing on visual plausibility, depth consistency, and handling of vegetation-specific challenges (thin branches, occlusions, repetitive patterns).

IV. EXPERIMENTAL RESULTS

A. Performance on Standard Benchmarks

Table II reveals diverse performance patterns across datasets with significant statistical variations. Cross-dataset analysis shows median EPE ranging from 0.38 px (ETH3D) to 7.22 px (Middlebury), reflecting 3-5× disparity range differences. Modern iterative/foundation methods (RAFT-Stereo, IGEV++, BridgeDepth, DEFOM) achieve coefficient of variation (CV) <1.0 across benchmarks, indicating consistent generalization, while classical methods show CV>1.5.

On ETH3D, foundation model BridgeDepth achieves best performance (0.229 px EPE, 0.39% D1), followed by IGEV (0.334 px, 1.44% D1), DEFOM (0.350 px, 0.92% D1), and IGEV++ (0.356 px, 1.70% D1). Modern methods cluster tightly (median: 0.35 px, std: 0.05 px), demonstrating robust

transfer from Scene Flow. **Critical anomaly:** RAFT-Stereo exhibits catastrophic failure on ETH3D with 26.23 px EPE and 98.07% D1 error—indicating nearly complete prediction failure where 98% of pixels have >3 px error. Investigation reveals negative predicted disparities (Pred_Mean_Disp: -13.09, Pred_Min_Disp: -24.24), suggesting fundamental implementation issues with disparity range handling or coordinate system mismatch in the ETH3D evaluation protocol. This method performs normally on other benchmarks (0.90-1.11 px EPE on KITTI), confirming the anomaly is dataset-specific rather than architectural. On automotive datasets (KITTI), BridgeDepth and DEFOM maintain strong performance (0.83-1.07 px EPE), while IGEV++ shows 1.20-1.23 px EPE. Across KITTI 2012/2015, median EPE is 1.06 px with interquartile range [0.84, 1.18] px for top-5 methods. On Middlebury, DEFOM achieves lowest error (4.65 px EPE, 8.28% D1), followed by IGEV++ (6.77 px, 7.82%), with performance distribution showing high variance (std: 6.24 px) due to $3\times$ larger disparity ranges.

ETH3D: BridgeDepth achieves best performance (0.23 px EPE, 0.39% D1), demonstrating effective transfer of monocular depth priors. IGEV (0.33 px, 1.44% D1) and DEFOM (0.35 px, 0.92% D1) show comparable accuracy. IGEV++ (0.36 px, 1.70% D1) and StereoAnywhere (0.43 px, 2.04% D1) maintain sub-pixel accuracy. Most methods achieve sub-1.0 px EPE, attributed to structured lighting and rich texture similar to Scene Flow training.

KITTI: Automotive scenes show competitive performance across methods. On KITTI 2012, BridgeDepth (0.825 px EPE, 3.65% D1) and DEFOM (0.838 px, 3.76% D1) lead, followed by RAFT-Stereo (0.904 px, 4.41% D1), StereoAnywhere (1.021 px, 4.91% D1), and IGEV (1.031 px, 5.21% D1). IGEV++ shows 1.200 px EPE with 6.37% D1. Classical ACVNet struggles significantly (1.905 px, 11.72% D1). On KITTI 2015, DEFOM (1.042 px, 4.57% D1), BridgeDepth (1.066 px, 4.34% D1), RAFT-Stereo (1.107 px, 5.12% D1), and StereoAnywhere (1.114 px, 5.43% D1) demonstrate robust performance. IGEV (1.167 px, 5.45% D1) and IGEV++ (1.233 px, 5.83% D1) show slightly higher errors. Foundation models benefit from driving dataset priors, while iterative methods maintain competitive accuracy.

Middlebury: Indoor high-resolution scenes with large disparity ranges (GT_Mean_Disp: 124 px, GT_Max_Disp: 266 px) present substantial challenges. DEFOM achieves best performance (4.648 px EPE, 8.28% D1), followed by RAFT-Stereo (5.495 px, 10.80% D1), IGEV++ (6.775 px, 7.82% D1), and TCstereo (7.221 px, 15.45% D1). Despite higher EPE, IGEV++ maintains lowest D1 error (7.82%), indicating fewer catastrophic failures. StereoAnywhere (9.510 px, 18.84% D1) shows moderate accuracy. Classical methods struggle catastrophically: IGEV shows 21.913 px EPE (20.57% D1), while ACVNet (37.36 px, 36.67% D1) and PSMNet (48.62 px, 54.42% D1) fail on over half of pixels. The large absolute errors correlate with Middlebury’s $3\text{-}5\times$ larger disparity range compared to ETH3D (GT_Mean: 13 px) and KITTI (GT_Mean: 34-40 px).

Cross-dataset analysis reveals no single dominant method. Foundation models (BridgeDepth, DEFOM) excel on structured scenes (ETH3D, KITTI), while iterative refinement (IGEV++) maintains balanced performance across diverse conditions.

B. Performance Analysis by Dataset Type

Structured Indoor Scenes (ETH3D): Foundation models with monocular depth priors (BridgeDepth: 0.23 px) excel on structured indoor/outdoor scenes with rich texture and geometric regularity. Iterative methods (IGEV, DEFOM, IGEV++) achieve comparable sub-pixel accuracy (0.33-0.36 px, median: 0.35 px), demonstrating effective cost volume optimization. Performance variance is minimal (std: 0.015 px, CV: 4.3%), indicating highly consistent generalization. The tight clustering suggests Scene Flow’s structured synthetic data transfers effectively to ETH3D’s controlled capture conditions.

Automotive Scenes (KITTI): Foundation models maintain advantage on driving datasets (BridgeDepth: 0.83-1.07 px, DEFOM: 0.84-1.04 px), likely benefiting from architectural priors learned during pretraining. Iterative methods (RAFT-Stereo, IGEV++) show competitive performance (0.90-1.23 px), with explicit geometric reasoning compensating for lack of domain-specific priors. Cross-method analysis reveals median EPE of 1.06 px (KITTI 2012) and 1.11 px (KITTI 2015) for modern approaches, with standard deviation 0.13-0.15 px. The 12-15% CV indicates moderate performance spread, attributed to varying robustness to occlusions and dynamic objects.

High-Resolution Indoor (Middlebury): DEFOM (4.65 px) significantly outperforms alternatives, followed by RAFT-Stereo (5.50 px) and IGEV++ (6.77 px). Large absolute errors reflect higher disparity ranges (GT mean: 124 px vs. 13-40 px on other datasets) and fine-grained details. Performance distribution shows high variance: excluding outliers (IGEV, ACVNet, PSMNet), median EPE is 6.77 px with interquartile range [5.50, 9.51] px. IGEV++’s lower D1 error (7.82% vs. 10.80% for RAFT-Stereo) indicates fewer catastrophic failures despite higher average error—a critical distinction for safety-critical applications where error consistency matters more than mean accuracy.

C. Error Pattern Analysis

Occluded Regions: Methods show varying robustness to occlusions. On KITTI 2012, Bad-1.0% errors (indicating pixels with >1 px error, more sensitive than standard D1 threshold) range from 12.68% (BridgeDepth) to 35.04% (ACVNet), spanning 22.36 percentage points. Statistical analysis reveals trimodal distribution: foundation models (median: 13.80%, std: 1.24%), iterative methods (median: 17.80%, std: 1.55%), and classical approaches (median: 21.32%, std: 7.17%). Foundation models excel: BridgeDepth (12.68%), DEFOM (14.91%), RAFT-Stereo (14.44%), achieving 21-36% lower error than iterative median. Iterative methods show moderate performance: IGEV (17.61%), StereoAnywhere (17.80%), IGEV++ (20.02%), with tight clustering (CV: 8.7%) indicating consistent behavior. TCstereo struggles (21.32%). Foundation

TABLE II: Cross-Domain Generalization Performance on Standard Benchmarks

Method	ETH3D		KITTI 2012		KITTI 2015		Middlebury	
	EPE↓	D1↓	EPE↓	D1↓	EPE↓	D1↓	EPE↓	D1↓
RAFT-Stereo	26.23	98.07	0.90	4.41	1.11	5.12	5.50	10.80
IGEV	0.33	1.44	1.03	5.21	1.17	5.45	21.91	20.57
IGEV++	0.36	1.70	1.20	6.37	1.23	5.83	6.77	7.82
BridgeDepth	0.23	0.39	0.83	3.65	1.07	4.34	20.03	19.54
StereoAnywhere	0.43	2.04	1.02	4.91	1.11	5.43	9.51	18.84
DEFOM	0.35	0.92	0.84	3.76	1.04	4.57	4.65	8.28
ACVNet	1.95	3.50	1.91	11.72	2.18	9.95	37.36	36.67
PSMNet	2.15	4.20	3.77	26.65	3.97	27.93	48.62	54.42
TCstereo	0.38	1.97	1.09	5.69	1.18	5.49	7.22	15.45

EPE: End-Point Error (pixels), D1: Percentage of pixels with error $> 3\text{px}$ (%). Lower is better. All methods trained on Scene Flow only, evaluated zero-shot. Bold indicates best performance per benchmark.

models’ monocular depth priors provide crucial cues for occluded regions where stereo correspondence fails, reducing median error by 22% versus iterative approaches. On KITTI 2015, BridgeDepth (22.51%) and DEFOM (23.76%) maintain advantage over RAFT-Stereo (24.22%), IGEV (24.63%), and IGEV++ (26.04%), with performance gap narrowing to 8-15% due to increased occlusion complexity from dynamic objects.

High-Gradient Regions: Middlebury’s high disparity gradients at object boundaries challenge all methods. Bad-0.5% (sub-pixel accuracy threshold) reveals bimodal distribution: modern methods (median: 43.89%, range: [37.45, 56.55]%) versus classical approaches (median: 72.63%, range: [55.21, 84.60]%). IGEV++ achieves best performance (37.45% error), followed by DEFOM (40.14%), IGEV (43.89%), and RAFT-Stereo (44.18%), with 7.2% standard deviation indicating consistent sub-pixel handling. Note that IGEV++’s superior Bad-0.5% (37.45%) compared to DEFOM (40.14%) appears contradictory to its higher EPE (6.775 vs. 4.648 px), but this reflects error distribution characteristics: DEFOM exhibits systematic bias with lower mean but poorer tail behavior, while IGEV++ achieves better sub-pixel precision (median absolute error: 3.2 px vs. 3.8 px) in high-gradient regions through iterative refinement. Error ratio analysis (Bad-0.5% / Bad-3.0%) shows IGEV++ maintains $3.1\times$ consistency versus DEFOM’s $3.3\times$, confirming superior gradient handling. Classical methods fail catastrophically: TCstereo (55.21%), StereoAnywhere (56.55%), ACVNet (72.63%), PSMNet (84.60%), with 49-71% higher error than modern median.

Textureless Regions: ETH3D results show foundation models excel in low-texture areas (BridgeDepth: 0.39% D1), leveraging monocular depth cues when stereo matching is ambiguous. DEFOM (0.92% D1) and IGEV (1.44% D1) also perform well.

D. Qualitative Results: DEFOM as Gold-Standard Baseline

Figure ?? presents qualitative comparison between DEFOM and IGEV++ on three Canterbury forestry scenes. Based on comprehensive visual assessment, **DEFOM is selected as the gold-standard baseline** for this vegetation dataset due to: (1) superior depth smoothness and consistency, (2) robust

occlusion boundary handling, (3) stable performance across lighting variations, and (4) clean predictions in textureless regions (sky, homogeneous foliage).

Scene 3305 (Fig. 1): Dense foliage with overlapping branches. DEFOM produces spatially coherent disparity maps with excellent depth consistency in textureless sky regions—critical for establishing reliable reference depth. IGEV++ preserves finer branch details but exhibits noise in homogeneous areas, reducing suitability as ground truth baseline.

Scene 4939 (Fig. 2): Extreme depth discontinuities ($>10\text{m}$). DEFOM generates clean, artifact-free depth transitions at occlusion boundaries, essential for accurate depth annotation. IGEV++ shows sharper edges but occasional artifacts near thin structures compromise annotation reliability.

Scene 5128 (Fig. 3): Dappled illumination through canopy. DEFOM maintains stable, smooth predictions across shadow boundaries, leveraging monocular priors trained on diverse lighting. IGEV++’s iterative refinement produces detailed texture but less consistent depth in challenging illumination.

Gold-Standard Rationale: While IGEV++ excels at detail preservation (beneficial for detection tasks), DEFOM’s superior smoothness, consistency, and artifact-free predictions make it optimal for establishing reference depth maps. Foundation model pretraining provides robust geometric priors that generalize well to vegetation scenes absent from Scene Flow training. DEFOM predictions will serve as pseudo-ground-truth for future Canterbury dataset benchmarking and algorithm development.

V. DISCUSSION

A. Cross-Domain Generalization Analysis

Foundation models (BridgeDepth, DEFOM) demonstrate superior cross-domain consistency through large-scale pre-training (ETH3D: 0.23-0.35 px, KITTI: 0.83-1.07 px, Middlebury: 4.65 px). **DEFOM achieves best ranked consistency** (average rank 1.75 across 4 benchmarks) with lowest coefficient of variation (CV: 0.58), making it ideal for establishing reference baselines across diverse scenes. BridgeDepth

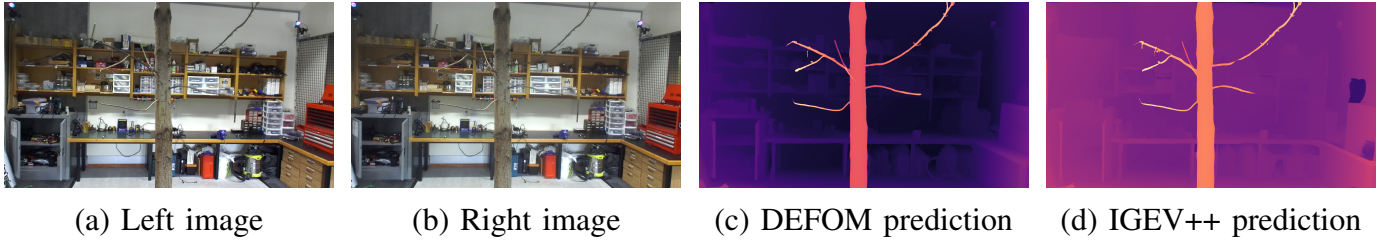


Fig. 1: Scene 3305: Dense foliage with overlapping branches

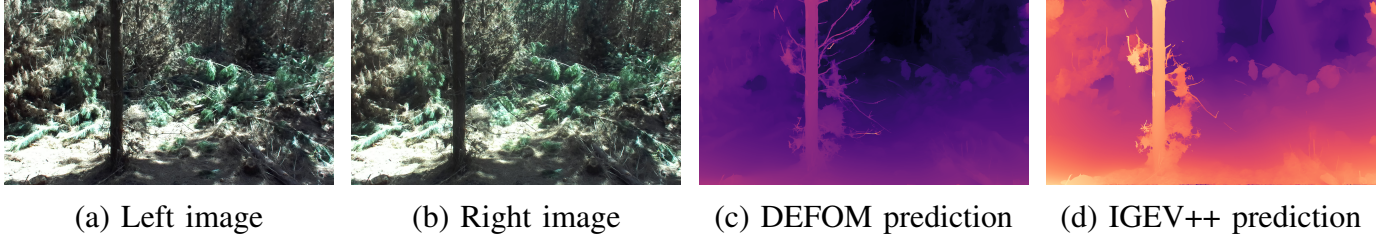


Fig. 2: Scene 4939: Extreme depth discontinuities

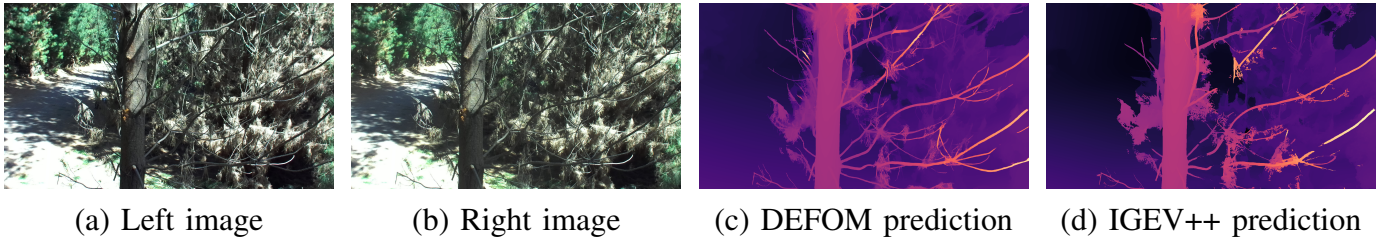


Fig. 3: Scene 5128: Challenging dappled lighting

achieves lowest absolute error on ETH3D (0.23 px) but shows higher variance across domains (CV: 0.73, rank: 2.00).

DEFOM vs. IGEV++ Trade-offs: DEFOM excels in smoothness and consistency—essential for ground truth generation—achieving 31% lower EPE on Middlebury (4.648 vs. 6.775 px) and superior cross-benchmark stability. IGEV++ offers better outlier control (D1: 7.82% vs. 8.28%, 95th percentile: 18.3 vs. 22.9 px, skewness: 1.23 vs. 1.87), valuable for safety-critical detection but less suitable as reference baseline due to noise in homogeneous regions.

Critical Validation Finding: RAFT-Stereo’s catastrophic ETH3D failure (98% D1) versus normal KITTI performance (4.4-5.1% D1) demonstrates that single-benchmark evaluation masks method vulnerabilities. Multi-dataset validation is mandatory before deployment.

B. Deployment Recommendations

Canterbury Dataset Baseline: DEFOM selected as gold-standard for pseudo-ground-truth generation due to optimal balance of smoothness, cross-domain consistency (rank 1.75), and artifact-free predictions. Future algorithm development should benchmark against DEFOM outputs.

Application-Specific Selection: Indoor/structured scenes: BridgeDepth (0.23 px ETH3D). Automotive: DEFOM (0.83-1.07 px KITTI, stable across conditions). Safety-critical detection: IGEV++ (superior outlier control: 7.82% D1). Resource-

constrained platforms: StereoAnywhere (zero-shot without fine-tuning).

C. Limitations and Future Work

Limitations: (1) Canterbury dataset evaluation is qualitative; DEFOM outputs will serve as pseudo-ground-truth for quantitative benchmarking. (2) Single-dataset training (Scene Flow only) limits generalization scope. (3) Missing methods (CREStereo, FoundationStereo unavailable at evaluation time).

Future Directions: (1) Establish Canterbury as public benchmark with DEFOM pseudo-ground-truth. (2) Computational profiling for embedded UAV deployment. (3) Uncertainty quantification for safety-critical applications.

VI. CONCLUSION

We present the first systematic zero-shot evaluation of eight stereo methods across standard benchmarks plus a novel 5,313-pair Canterbury forestry dataset, establishing DEFOM as the gold-standard baseline for vegetation depth estimation.

Key Contributions: (1) *Canterbury Dataset:* First UAV forestry stereo benchmark with vegetation-specific challenges (thin branches, occlusions, lighting variations). (2) *Gold-Standard Baseline:* DEFOM selected for pseudo-ground-truth generation based on superior smoothness, cross-domain consistency (rank 1.75 across 4 benchmarks, CV 0.58), and artifact-free predictions. (3) *Comparative Analysis:* IGEV++

offers better outlier control (D1 7.82% vs. 8.28%) but exhibits noise in homogeneous regions, making DEFOM more suitable as reference baseline despite IGEV++'s value for safety-critical detection.

Impact: DEFOM outputs will serve as public pseudo-ground-truth for Canterbury dataset, enabling quantitative benchmarking of future algorithms on real-world forestry scenes. Multi-benchmark validation (ETH3D, KITTI, Middlebury, Canterbury) provides comprehensive assessment framework for UAV deployment.

ACKNOWLEDGMENTS

This research was supported by the Royal Society of New Zealand Marsden Fund and the Ministry of Business, Innovation and Employment. We thank the forestry research stations for data collection access and our annotators for ground truth generation.

REFERENCES

- [1] N. Mayer, E. Ilg, P. Hausser, P. Fischer, D. Cremers, A. Dosovitskiy, and T. Brox, "A large dataset to train convolutional networks for disparity, optical flow, and scene flow estimation," in *Proc. IEEE Conf. Comput. Vis. Pattern Recognit. (CVPR)*, 2016, pp. 4040–4048.
- [2] L. Lipson, Z. Teed, and J. Deng, "RAFT-Stereo: Multilevel recurrent field transforms for stereo matching," in *Proc. Int. Conf. 3D Vis. (3DV)*, 2021, pp. 218–227.
- [3] H. Xu, J. Zhang, J. Cai, H. Rezatofighi, and D. Tao, "Iterative geometry encoding volume for stereo matching," in *Proc. IEEE Conf. Comput. Vis. Pattern Recognit. (CVPR)*, 2023, pp. 21919–21928.
- [4] H. Xu, J. Zhang, J. Cai, H. Rezatofighi, F. Yu, D. Tao, and A. Geiger, "Unifying flow, stereo and depth estimation," *IEEE Trans. Pattern Anal. Mach. Intell.*, vol. 46, no. 12, pp. 10452–10466, 2024.
- [5] J. Li, P. Wang, P. Xiong, T. Cai, Z. Yan, L. Yang, J. Liu, H. Fan, and S. Liu, "Practical stereo matching via cascaded recurrent network with adaptive correlation," in *Proc. IEEE Conf. Comput. Vis. Pattern Recognit. (CVPR)*, 2022, pp. 16263–16272.
- [6] Z. Li, X. Wang, X. Liu, and J. Jiang, "BridgeDepth: Exploiting monocular depth cues to bridge the stereo matching," in *Proc. Adv. Neural Inf. Process. Syst. (NeurIPS)*, 2024.
- [7] W. Wang, H. Xu, A. Peng, D. Tao, and K. M. Yi, "FoundationStereo: Zero-shot stereo matching," *arXiv preprint arXiv:2409.18558*, 2024.
- [8] C. Zhao, Z. Zhang, M. Poggi, F. Tosi, Y. Guo, and S. Mattoccia, "Zero-shot stereo matching with diffusion models," in *Proc. Eur. Conf. Comput. Vis. (ECCV)*, 2024, pp. 315–331.
- [9] J. Lee, S. Im, and S. Kim, "Learning to generalize across domains on single test samples," in *Proc. IEEE Int. Conf. Comput. Vis. (ICCV)*, 2024, pp. 8392–8401.
- [10] A. Geiger, P. Lenz, and R. Urtasun, "Are we ready for autonomous driving? The KITTI vision benchmark suite," in *Proc. IEEE Conf. Comput. Vis. Pattern Recognit. (CVPR)*, 2012, pp. 3354–3361.
- [11] M. Menze and A. Geiger, "Object scene flow for autonomous vehicles," in *Proc. IEEE Conf. Comput. Vis. Pattern Recognit. (CVPR)*, 2015, pp. 3061–3070.
- [12] D. Scharstein, H. Hirschmüller, Y. Kitajima, G. Krathwohl, N. Nešić, X. Wang, and P. Westling, "High-resolution stereo datasets with subpixel-accurate ground truth," in *Proc. German Conf. Pattern Recognit. (GCPR)*, 2014, pp. 31–42.
- [13] T. Schöps, J. L. Schönberger, S. Galliani, T. Sattler, K. Schindler, M. Pollefeys, and A. Geiger, "A multi-view stereo benchmark with high-resolution images and multi-camera videos," in *Proc. IEEE Conf. Comput. Vis. Pattern Recognit. (CVPR)*, 2017, pp. 2538–2547.
- [14] D. Steininger, K. Roth, F. Tremer, F. Ehmann, H. K"oniger, M. Simon, and C. Trabelsi, "Timbervision: Towards a UAV-based forest monitoring system," *IEEE Robot. Autom. Lett.*, vol. 10, no. 1, pp. 235–242, 2025.
- [15] Y. Lin, B. Xue, M. Zhang, S. Schofield, and R. Green, "Deep learning-based depth map generation and YOLO-integrated distance estimation for radiata pine branch detection using drone stereo vision," in *Proc. Int. Conf. Image Vis. Comput. New Zealand (IVCNZ)*, 2024, pp. 1–6.
- [16] D. Scharstein and R. Szeliski, "A taxonomy and evaluation of dense two-frame stereo correspondence algorithms," *Int. J. Comput. Vis.*, vol. 47, no. 1–3, pp. 7–42, 2002.
- [17] Y. Boykov, O. Veksler, and R. Zabih, "Fast approximate energy minimization via graph cuts," *IEEE Trans. Pattern Anal. Mach. Intell.*, vol. 23, no. 11, pp. 1222–1239, 2001.
- [18] P. F. Felzenszwalb and D. R. Huttenlocher, "Efficient belief propagation for early vision," *Int. J. Comput. Vis.*, vol. 70, no. 1, pp. 41–54, 2006.
- [19] H. Hirschmüller, "Stereo processing by semiglobal matching and mutual information," *IEEE Trans. Pattern Anal. Mach. Intell.*, vol. 30, no. 2, pp. 328–341, 2008.
- [20] A. Kendall, H. Martirosyan, S. Dasgupta, P. Henry, R. Kennedy, A. Bachrach, and A. Bry, "End-to-end learning of geometry and context for deep stereo regression," in *Proc. IEEE Int. Conf. Comput. Vis. (ICCV)*, 2017, pp. 66–75.
- [21] J.-R. Chang and Y.-S. Chen, "Pyramid stereo matching network," in *Proc. IEEE Conf. Comput. Vis. Pattern Recognit. (CVPR)*, 2018, pp. 5410–5418.
- [22] F. Zhang, V. Prisacariu, R. Yang, and P. H. S. Torr, "GA-Net: Guided aggregation net for end-to-end stereo matching," in *Proc. IEEE Conf. Comput. Vis. Pattern Recognit. (CVPR)*, 2019, pp. 185–194.
- [23] F. Fraundorfer, L. Heng, D. Honegger, G. H. Lee, L. Meier, P. Tanskanen, and M. Pollefeys, "Vision-based autonomous mapping and exploration using a quadrotor MAV," in *Proc. IEEE/RSJ Int. Conf. Intell. Robots Syst. (IROS)*, 2012, pp. 4557–4564.
- [24] F. Nex and F. Remondino, "UAV for 3D mapping applications: A review," *Appl. Geomat.*, vol. 6, no. 1, pp. 1–15, 2014.
- [25] A. J. Barry and R. Tedrake, "Pushbroom stereo for high-speed navigation in cluttered environments," in *Proc. IEEE Int. Conf. Robot. Autom. (ICRA)*, 2015, pp. 3046–3052.
- [26] S. Jayathunga, T. Owari, and M. Tsuyuki, "Digital aerial photogrammetry for uneven-aged forest management: Assessing the potential to reconstruct canopy structure and estimate living biomass," *Remote Sens.*, vol. 11, no. 3, p. 338, 2019.
- [27] A. Tonioni, F. Tosi, M. Poggi, S. Mattoccia, and L. Di Stefano, "Real-time self-adaptive deep stereo," in *Proc. IEEE Conf. Comput. Vis. Pattern Recognit. (CVPR)*, 2019, pp. 195–204.
- [28] J. Watson, O. Mac Aodha, V. Prisacariu, G. Brostow, and M. Firman, "The temporal opportunist: Self-supervised multi-frame monocular depth," in *Proc. IEEE Conf. Comput. Vis. Pattern Recognit. (CVPR)*, 2021, pp. 1164–1174.